

Introduction

Realization of the future Comprehensive Nuclear Test Ban Treaty (CTBT) will require ensuring its compliance, making the CTBT a prime example of forensic seismology. Following indications of a nuclear explosion obtained on the basis of the (IMS) monitoring network further evidence needs to be sought at the location of the suspicious event. For such an On-Site Inspection (OSI) at a possible nuclear test site the treaty lists several techniques that can be carried out by the inspection team, including aftershock monitoring and the conduction of active seismic surveys. While those techniques are already well established, a third group of methods labeled as "resonance seismometry" is less well defined and needs further elaboration.

A prime structural target that is expected to be present as a remnant of an underground nuclear explosion is a cavity at the location and depth the bomb was fired. As example, Fig. 1 a) shows the layout of the central zone from an underground nuclear test at the Balapan test site in Semipalatinsk as given by Adushkin and Spivak (2004). The cavity has a diameter of ~ 60 m and is in a depth of 200 m under the surface. Originally "resonance seismometry" referred to resonant seismic emission of the cavity within the medium that could be stimulated by an incident seismic wave of the right frequency and observed as peaks in the spectrum of seismic stations in the vicinity of the cavity. However, it is not yet clear which are the conditions for which resonant emissions of the cavity could be observed. In the meantime the usage of the term "resonance seismometry" in CTBT research has been extended to indicate particular characteristics of seismic signals and noise emerging from the anomalous zone, which may be picked up directly, or as variation with distance or time. Nevertheless, we focus here on the resonance itself.

In order to define distance-, frequency- and amplitude ranges at which resonant emissions can be observed, we study the interaction of seismic waves with underground cavities, and we use the generic model of a spherical acoustic cavity in an elastic full-space, as shown in Fig. 1b).

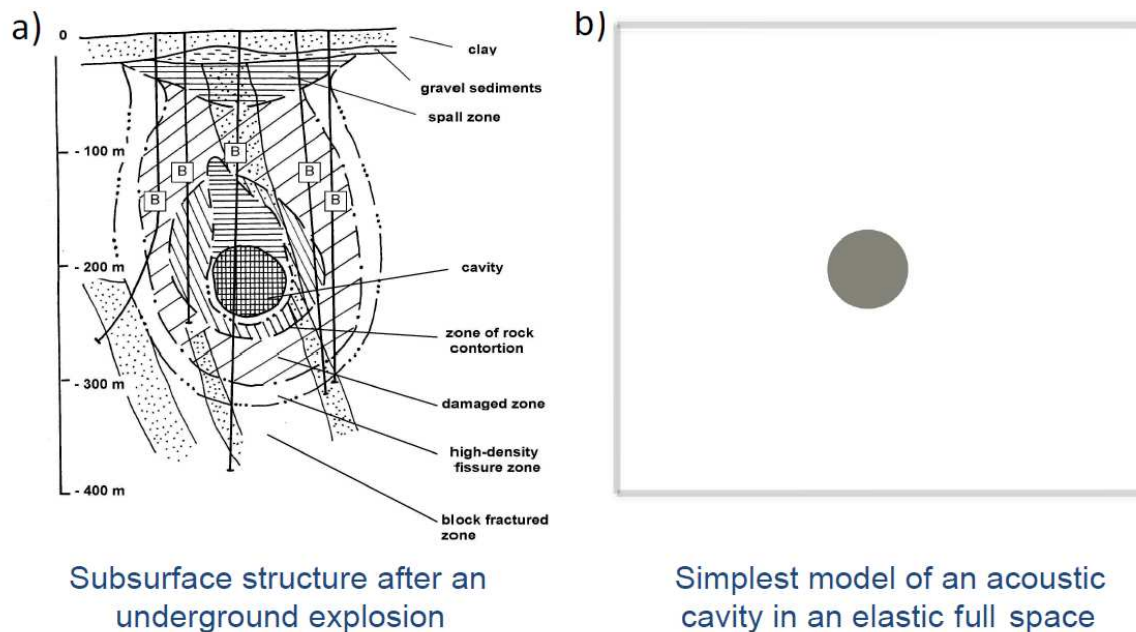


Figure 1 Representations of cavities from underground nuclear explosions: a) realistic geological model from the Semipalatinsk test site (in Kazakhstan), b) generic model of an acoustic sphere in an elastic full space used to study resonances.

Analytical derivation of the full wavefield

To solve the forward problem for the full elastic wavefield around acoustic spherical inclusions, we use an analytical solution developed for incidence of plane P- and S- waves at a spherical cavity (Korneev, 1996). This solution solves the time-harmonic problem, that is, the scattered displacement field outside and inside the cavity for a plane incident wave is derived for fixed frequencies.

Example calculations for a fluid-filled acoustic cavity and an incident P-wave in Z-direction with slightly different frequency (14 Hz and 15 Hz) are shown in Fig. 2 for two different acoustic inclusion. Since the incident P-wave is running in the positive Z-direction, upper and lower half-spaces of panels c)-f) describe the total wavefields including transmitted and back-scattered waves, respectively. The surrounding medium is for all calculations the same. The parameters for the acoustic cavity are chosen to resemble either a fluid-filled or a gas-filled cavity. The radius of the cavity is fixed to 30 m. The model parameters are chosen as follows:

Surrounding elastic medium (model 1 and model 2):

$$v_p = 6.0 \text{ km/s} \quad v_s = 3.5 \text{ km/s}. \quad \rho = 2700.0 \text{ kg/m}^3$$

Fluid-filled acoustic cavity (model 1):

$$v_p = 1.4 \text{ km/s} ; \rho_1 = 1000.0 \text{ kg/m}^3$$

Gas-filled acoustic cavity (model 2):

$$v_p = 0.3 \text{ km/s} ; \rho_1 = 1.5 \text{ kg/m}^3.$$

While the incident wavefields (upper panels a and b) for 14 Hz and 15 Hz, are very similar, the associated total fields for a fluid-filled inclusion (panels c and d) show different behaviour: for a 14 Hz incident P-wave the total field resembles the incident field with minor changes whereas in the case of a 15 Hz incident P-wave the total field is strongly perturbed by the presence of the fluid-filled acoustic cavity. In contrast to this observation, the total fields for a gas-filled inclusion (panels e and f) resemble each other in the surrounding medium. Only inside the gas-filled cavity they show a different pressure field, but which would be not observable from the outside.

Scattering cross-sections

To compare the energy flux of incident and scattered wave fields scattering cross-sections are derived from the analytical solution. They are defined as the relation of the integrated scattered energy flow F_{sc} and the integrated incident energy flow F_{inc} through a surface that completely surrounds the cavity. They define a scalar value for each frequency for the scattered P- and S- wavefields.

Figure 3 shows scattering cross-sections for the two different acoustic inclusion as a function of frequency and the dimensionless parameter $k_p R$, which equals the ratio of the cavity circumference and the wavelength of a P-wave (U/λ). The model parameters are chosen to be the same as for the full wavefield derivation shown in Fig. 2. The scattering cross-section of the fluid-filled cavity (in Fig. 3a) shows strong resonances at 15 Hz or $0.41 k_p R$ and 32.75 Hz or $1.03 k_p R$. The first peak at 15 Hz is mainly caused by scattered S-waves, while the second peak is mainly caused by scattered P-wave. Moreover, many smaller resonance peaks are observed throughout the whole displayed frequency range. In contrast, the scattering cross-section of a gas-filled inclusion (Fig 3b) looks like a smoothed version of the scattering cross-section of the fluid-filled inclusion. It does not show any resonant peaks and resembles the case of an vacuum inclusion, shown by Korneev (1996). However it is interesting, that the scattered energy consists to a larger part of S-waves for $k_p R < 3$, which corresponds in the dimensions of a cavity from an underground nuclear test to frequencies up to 95 Hz. The total scattered energy shows an increase from 12 Hz to 50 Hz and remains constant for higher frequencies. For both, fluid-filled and gas-filled cavities, the total scattered energy goes to zero for small frequencies.

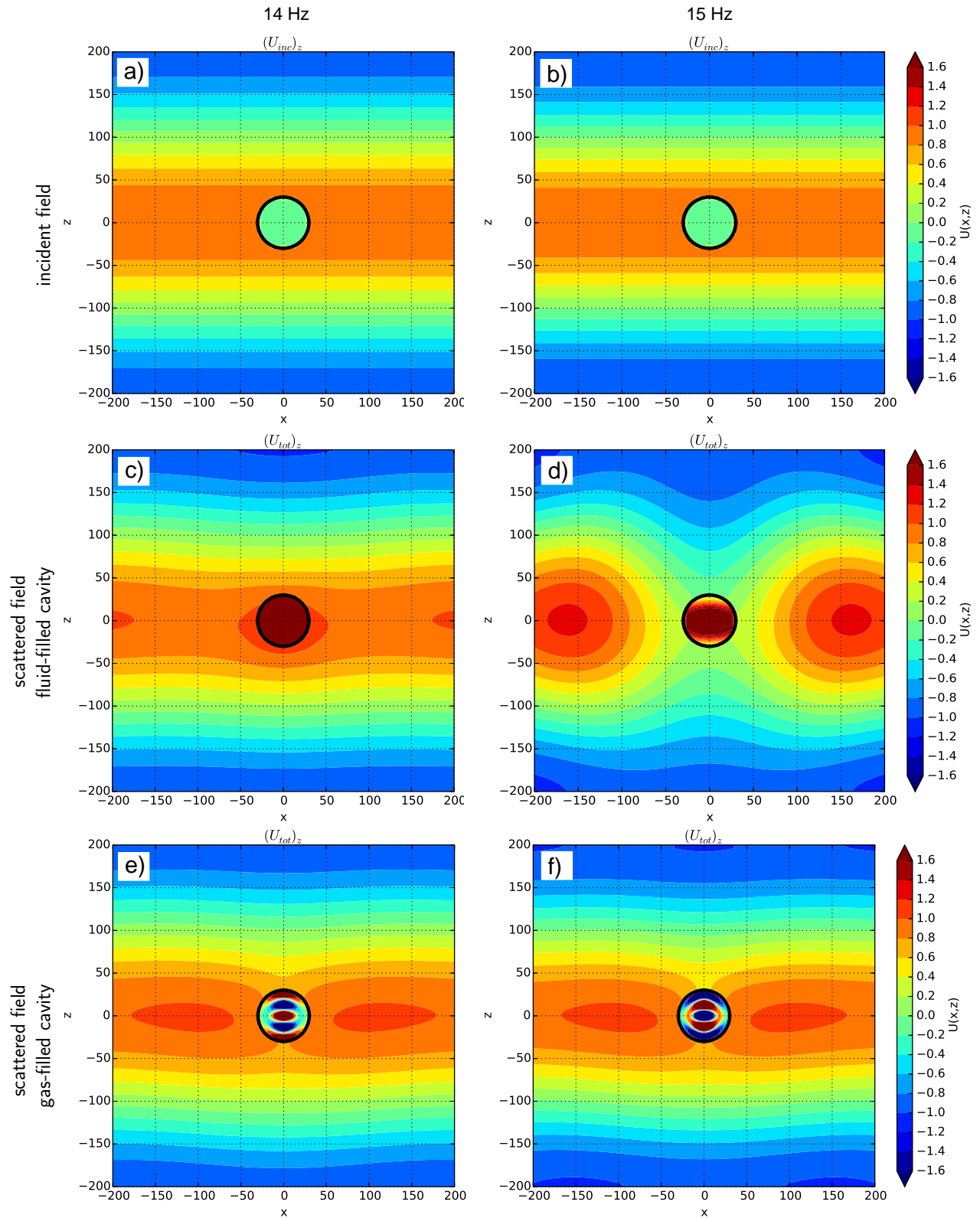


Figure 2 Full wavefield of incident and total field for a plane wave incident wave at a fluid-filled acoustic cavity. In the left panels a), c) and e) the frequency of the harmonic incident wave is 14 Hz, while in the right panels b), d) and f) it is 15 Hz. All panels show Z-components Panels in a) and b) for the incident fields, in c) and d) for the total (incident + scattered) fields for a fluid-filled cavity and in e) and f) for the total field for a gas-filled cavity.

Conclusions

We use the analytical exact solution for plane elastic wave interaction with a spherical acoustic inclusion derived by Korneev (1996) to derive the full wavefield scattered from a cavity in the geometrical dimensions of one created by underground nuclear explosions. For a fluid-filled cavity small changes of the frequency can cause strong variations of the scattered field. These resonances are displayed through scattering cross-sections for a fluid-filled spherical cavity. In the geometrical dimensions of a cavity from the nuclear explosion these resonances would appear at around 15 and 30 Hz and are thus in an observable frequency range. This would apply for the case that the cavity is filled by ground water after the explosion as reported by Martinez et al. (1999). However, in the case of a gas-filled acoustic cavity no resonances are observed. In this case the spectral characteristics of the cavity can be described by an increase of scattered energy with frequency and a dominance of scattered S-waves energy for frequencies smaller than 95Hz.

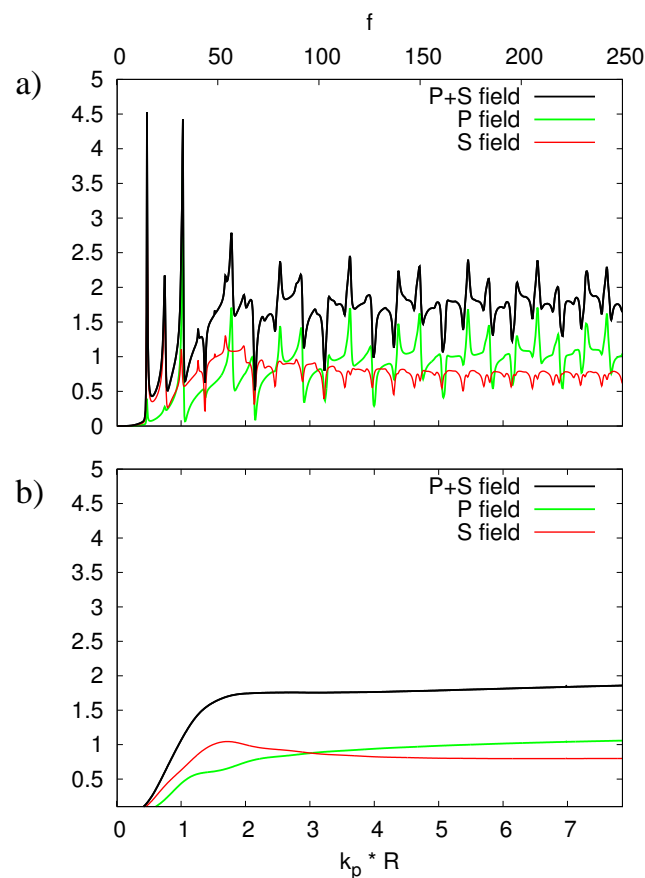


Figure 3 Scattering cross-sections for acoustic inclusions: a) fluid filled-acoustic inclusion, b) gas-filled acoustic inclusion.

References

Adushkin, V. V. and Spivak, A. A. [2004] Changes in Properties of Rock Massifs Due to Underground Nuclear Explosions. *Combustion, Explosion, and Shock Waves* Vol. 40, No. 6, 624-634.

Korneev, V. A. Johnson, L. R. [1996] Scattering of P and S Waves by a Spherically Symmetric Inclusion. *Pageoph*, Vol. 147, No. 4, 675-718.

Martinez B.A., Finnegan D.L., Thompson J.L., Kung K.S. [1999] Laboratory and field studies related to radionuclide migration at the Nevada test site. Los Alamos National Lab, Los Alamos